

Article

Concise Robust Control of the Nonlinear Ship in Course-Keeping Control

Changjun Zou *, Jia Yu and Yingxuan Guo

School of Information Engineering, East China Jiaotong University, Nanchang 330013, China; 2612@ecjtu.edu.cn or 3262@ecjtu.edu.cn (J.Y.); 2018031002000202@ecjtu.edu.cn (Y.G.)

* Correspondence: zoucj2006@163.com or zouchangjun@ecjtu.edu.cn

Abstract: Most of the existing nonlinear ship course-keeping control systems are designed with the Nomoto model, which solely considers the yawing of the ship with only one Degree of Freedom (DOF), and it does not consider the coupling between the longitudinal and the lateral velocity of the ship. In this paper, a nonlinear ship course controller design method that can be used in a nonlinear coupled model was proposed. A stable nonlinear ship course controller with anti-wind and anti-wave interference was constructed based on the Lyapunov stability principle and robust control theory, which can be used in the course control of autopilot in the case of wind and waves. In this method, the coupling among the longitudinal and lateral velocity as well as yawing of the ship was considered. The simulation results showed that the method can not only effectively control the ship's course but also can track the dynamic course effectively. At the same time, compared with the PID control method based on backstepping, the steering angle of the rudder angle of our method is smaller and the wear and tear of steering gear will be smaller.

Keywords: course-keeping control; nonlinear ship control; concise robust control; Lyapunov stability



Citation: Zou, C.; Yu, J.; Guo, Y. Concise Robust Control of the Nonlinear Ship in Course-Keeping Control. *Appl. Syst. Innov.* **2021**, *4*, 35. <https://doi.org/10.3390/asi4020035>

Academic Editor: Ondrej Krejcar

Received: 7 April 2021
Accepted: 17 May 2021
Published: 21 May 2021

Publisher's Note: MDPI stays neutral with regard to jurisdictional claims in published maps and institutional affiliations.



Copyright: © 2021 by the authors. Licensee MDPI, Basel, Switzerland. This article is an open access article distributed under the terms and conditions of the Creative Commons Attribution (CC BY) license (<https://creativecommons.org/licenses/by/4.0/>).

1. Introduction

Autopilot is a piece of indispensable and vital equipment for ship maneuvering nowadays. With the improvement of navigation safety requirements and the growth of transportation demand, the requirements for autopilot are also increasing rapidly. The appearance of autopilot is a milestone in the field of navigation. It has led to the expectation to eliminate heavy manual labor and to realize automatic control in ship handling. Early mechanical autopilot can only carry out simple proportional control. It needs to select low gain for the sake of avoiding oscillation and it can only be used for low-precision course-keeping control.

In the 1950s, the second generation, with a more complex and efficient electromechanical autopilot, emerged, which is well known as the PID autopilot. Its course deviation provides a correction signal to the steering equipment in an autopilot; however, the PID control method is too sensitive to high-frequency interference such as wind and waves. The “dead zone” nonlinear regulation is often adopted for complex steering to avoid the oscillation in course caused by high-frequency interference. Nevertheless, the dead zone often leads to the deterioration of the low-frequency characteristics for the control system, resulting in continuous periodic yawing, which will cause the deterioration of navigation accuracy, an increase in energy consumption, and the aggravation of rudder wear [1] Compared with the first generation of autopilot, the second generation of autopilot has made great progress, but it still cannot adapt to changes in the working conditions and working environment of the ship. Therefore, the steering operation is too frequent, the steering rudder angle is large, and the energy consumption and wear and tear of the steering gear are significant.

In the 1970s, due to the development of adaptive control theory and the progress of computer technology, researchers began to discuss the possibility of introducing adaptive

control theory into ship automatic control. Under their unremitting efforts, the third generation of adaptive autopilot products was born [2,3]. Adaptive control [4,5] is a dynamic control method that can continuously and automatically identify the parameters of the target system, and the algorithm could adapt the ship to varying environmental conditions. Adaptive control mainly includes the adaptive PID method, the random adaptive method [6], the model reference method [2,3], and the self-correction method [7,8]. However, the adaptive control method is not only related to the estimated value of the cost function but also depends on the accuracy of the disturbance model established in the controller. Adaptive autopilot has achieved certain results in improving control accuracy and reducing energy consumption. However, due to the high cost of physical implementation and difficulty in parameter adjustment, especially due to the nonlinearity and uncertainty of ship motion and sea state, it is difficult to guarantee the control performance in bad weather, and sometimes it even affects the stability of the system.

In recent years, with the continuous development of modern control theory and computer technology, various new control methods have been applied to the field of nonlinear ship course control, such as the feedback linearization [9], generalized predictive control [10,11], and LQR [12]/LQG [13] methods. However, these methods have higher requirements of the control target model, and some of them have difficulty guaranteeing the control performance due to the nonlinearity and uncertainty of the ship motion system.

For ship course control, it shows nonlinearity due to uncertain disturbances such as wind, wave, and current [14–16].

To solve the nonlinear and uncertain problems of ship course control, many nonlinear control technologies have been developed in ship course control. For instance, the ship course-keeping and track-keeping control based on sliding mode control [17–19] has certain robustness to system uncertainty and external disturbance, but the high-frequency oscillation phenomenon of sliding model control is difficult to resolve.

Furthermore, the nonlinear robust controller for ship course control has been proposed by introducing an integral item to eliminate the static error [20]. The stability of the course controller is guaranteed by the construction of the Lyapunov candidate function [21,22]. Nevertheless, the control target of this method only has one DOF in ship yawing and lacks the coupling of longitudinal and lateral velocity, so there is a limitation in its practical application. For nonlinear ship control, the μ -synthesis method has an advantage in terms of robustness, but it is difficult to determine the parameters in the controller [23], which limits its application in practical use.

While another method based on the Lyapunov candidate function has attracted much attention in the ship course control field [16,24,25], this method deals with the nonlinear term recursively and it is also capable of tracking the course for under-actuated ships with stochastic disturbances [26].

The contribution and novelty of our method:

1. A concise robust controller design method for a nonlinear 3DOF model based on the Lyapunov stability principle is proposed, and the method takes the longitudinal and the lateral velocity coupling into consideration. Our method is easy to implement with few parameters to determine.

2. The performance of our new method is verified on a 3DOF ship mode; the new method can achieve better steering performance with less rudder wear.

2. Basic Structure of Ship Course Control System

The basic structure of the ship course control system is shown in Figure 1. The structure of ship course control mainly includes a controller, steering gear model, ship motion mathematical model, wind wave, and other external interferences.

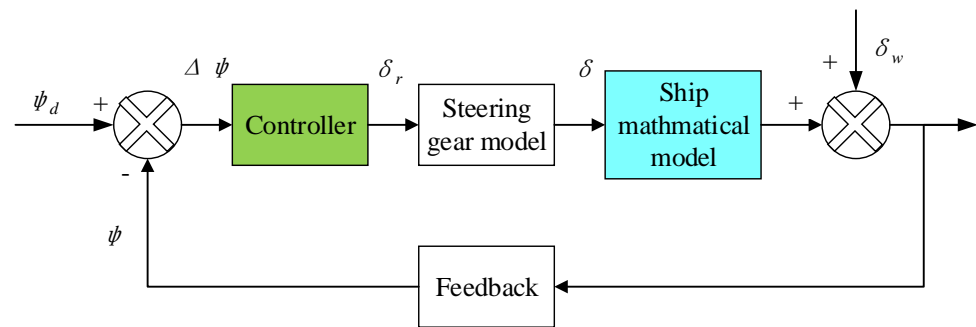


Figure 1. The basic structure for ship course control in simulation.

In Figure 1, ψ_d is the setting target course; ψ is the current course; $\Delta\psi$ is the course deviation between the target course and current course; δ_r is the control rudder angle output from the controller; δ is the rudder angle after considering the characteristic limitation of the steering gear; δ_w is the equivalent rudder angle of external interference such as wind and waves.

The basic process of ship course control mainly involves the following four steps:

(1) The rudder angle is applied to adjust the ship's course when the ship is sailing. The ship course control input is obtained by comparing the target course with the current course, and the controller output is calculated according to the control law design.

(2) Because the actual rudder angle output is limited by the characteristics of the steering gear, the limitation contains the maximum rudder angle limit and the rudder angular velocity limit. After the correction, the rudder angle output satisfying the characteristics of the steering gear is obtained, and the rectified rudder angle output is closer to reality after considering the characteristic limitation of the steering gear.

(3) The mathematical model of ship motion produces the corresponding yawing under the action of the input rudder angle, and the corresponding equivalent rudder angle output is obtained under the effect of external wind and wave interference; hence, the actual heading output is obtained after the superposition of the two. At this time, the output heading includes wind–wave interference. In this way, we can handle both the wind and wave via the equivalent input rudder angle, instead of dealing with the wind and wave themselves. This makes the control system more concise. For Beaufort scale 6, the wave disturbance model driven by Gaussian white noise is as below:

$$\psi_H = \frac{0.4198s}{s^2 + 0.3638s + 0.3675} w_H \quad (1)$$

where ψ_H , s , w_H are the Gaussian white noise, Laplace operator, and high-frequency wave disturbance, respectively. For more detailed information, please refer to reference [24,25].

(4) The actual course is fed back to the controller through the compass and other sensors. The variance is obtained by comparing with the target course; thus, the controller completes the closed-loop cycle.

From the basic structure of the ship course controller, it can be seen that the mathematical model and controller of ship motion are the core of the whole system. The mathematical model of ship motion is the mathematical abstraction of the actual ship, which reflects the dynamic and kinematic characteristics of the actual ship to a certain extent; hence, it can be regarded as an approximation of the actual ship. The controller is a device to calculate the control rudder angle according to the course deviation and control law designed. The performance of the controller directly affects the energy consumption of the ship and the wear and tear of the steering gear.

3. Mathematical Model of Ship Motion

The integrated modeling method of ship motion has a strict mathematical foundation. Because the interaction between various parts of the ship has been automatically taken into account in the hydrodynamic derivatives experiment, it has higher accuracy theoretically.

From the point of view of the Abkowitz nonlinear ship motion model, the third-order dynamic nonlinear model of the ship is developed from the Taylor series. The general expression of the hydrodynamic force of ship motion is stated as follows:

$$\begin{cases} m(\dot{u} - vr - x_G r^2) = X(\dot{u}, \dot{v}, \dot{r}, u, v, r, n, \delta) \\ m(\dot{v} + ur + x_G \dot{r}) = Y(\dot{u}, \dot{v}, \dot{r}, u, v, r, n, \delta) \\ I_{zz} \dot{r} + mx_G(\dot{v} + ur) = N(\dot{u}, \dot{v}, \dot{r}, u, v, r, n, \delta) \end{cases} \quad (2)$$

Among them, m is the mass of ship hull; $\dot{u}, \dot{v}, \dot{r}, u, v, r$ are the longitudinal acceleration, lateral acceleration, yawing angle acceleration, and the corresponding velocity components, respectively; n, δ is the propeller revolution and rudder angle, respectively; x_G are the distance between the hull center and the centerline; X, Y represent the longitudinal and lateral forces on the hull, respectively; N is the turning moment.

The above formula is expanded by the Taylor series near the equilibrium point, and the higher-order terms above the third order are ignored in the control design. In addition, the terms of rigid inertia force, fluid inertia force acting on the hull, lift, and resistance terms are substituted into the above formula; hence, the non-dimensional Abkowitz nonlinear mathematical model of ship motion is obtained:

$$\begin{cases} (m - X_{\dot{u}})\dot{u} = f_1(u, v, r, \delta)/0.5\rho L^3 \\ (m - X_{\dot{v}})\dot{v} = f_2(u, v, r, \delta)/0.5\rho L^3 \\ (mx_G - N_{\dot{v}})\dot{v} + (I_{zz} - N_{\dot{r}})\dot{r} = f_3(u, v, r, \delta)/0.5\rho L^4 \end{cases} \quad (3)$$

where:

$$\begin{aligned} f_1(u, v, r, \delta) = & X_0 + X_u \Delta u + X_{uu} \Delta u^2 + X_{uuu} \Delta u^3 + X_{vv} \Delta v^2 \\ & + (X_{rr} + mx_G) r^2 + X_{\delta\delta} \delta^2 + (X_{vr} + m)vr + X_{v\delta} v\delta \\ & + X_{r\delta} r\delta + X_{v\delta} v^2 \Delta u + X_{rru} r^2 \Delta u \\ & + X_{\delta\delta u} \delta^2 \Delta u + X_{vru} vr \Delta u + X_{v\delta u} v\delta \Delta u + X_{r\delta u} r\delta \Delta u \end{aligned} \quad (4)$$

$$\begin{aligned} f_2(u, v, r, \delta) = & Y_0 + Y_u \Delta u + Y_{uu} \Delta u^2 + Y_{uuu} \Delta u^3 + Y_v v + Y_r r + mru \\ & + Y_{\delta} \delta + Y_{vv} \Delta v^3 + Y_{rrr} \Delta r^3 + Y_{\delta\delta\delta} \delta^3 + Y_{vvr} v^2 r + Y_{v\delta} v^2 \delta \\ & + Y_{vrr} vr^2 + Y_{\delta rr} \delta r^2 + Y_{v\delta\delta} v\delta^2 + Y_{r\delta\delta} r\delta^2 + Y_{vr\delta} vr\delta + Y_{vu} v\Delta u \\ & + Y_{ru} r\Delta u + Y_{\delta u} \delta \Delta u + Y_{vu} v\Delta u^2 + Y_{ruu} r\Delta u^2 + Y_{\delta uu} \delta \Delta u^2 \end{aligned} \quad (5)$$

$$\begin{aligned} f_3(u, v, r, \delta) = & N_0 + N_u \Delta u + N_{uu} \Delta u^2 + N_{uuu} \Delta u^3 + N_v v + N_r r \\ & + N_{\delta} \delta + N_{vv} \Delta v^3 + N_{rrr} \Delta r^3 + N_{\delta\delta\delta} \delta^3 \\ & + N_{vvr} v^2 r + N_{v\delta} v^2 \delta + N_{vrr} vr^2 + N_{\delta rr} \delta r^2 \\ & + N_{v\delta\delta} v\delta^2 + N_{r\delta\delta} r\delta^2 + N_{vr\delta} vr\delta + N_{vu} v\Delta u \\ & + N_{ru} r\Delta u - mx_G r\Delta u + N_{\delta u} \delta \Delta u + N_{vu} v\Delta u^2 \\ & + N_{ruu} r\Delta u^2 + N_{\delta uu} \delta \Delta u^2 \end{aligned} \quad (6)$$

Among them are the hydrodynamics derivatives except for u, v, r, δ , which could be determined by experiments. Among the parameters on the right side, X, Y, N are hydrodynamic derivatives.

4. Design of a Nonlinear Robust Controller for Ship Course Control

4.1. Design of Concise Robust (CROB) Controller

H_{∞} robust control theory solves the problem of robust controller design for MIMO systems in the frequency domain. However, the whole design process is not only based on difficult mathematical theory but also requires many experiments to be carried out to choose the proper weight function to obtain a robust controller with better performance. Moreover,

the order of the controller obtained is always too high, which is a time-consuming task compared with the robustness of the controller; in other words, the price is too high.

Given the correlation between the mixed sensitivity algorithm and the compensation sensitivity function T and sensitivity function S in the robust control theory, G represents the transfer function for the system and K is the controller designed; the controller can be determined by constructing the four parameters related to compensation sensitivity function T , such as maximum singular value, bandwidth, closing-door slope, and closed-loop of peak spectrum. Because these four parameters are of engineering significance, the controller is designed in accordance with the closed-loop transfer function of the system. Because of the correlation between S and T , the shape of S can be determined indirectly once the shape of T is set up, and the robust performance and robust stability of the system are guaranteed. This method is called the closed-loop gain-forming algorithm, which is also named the concise robust control method.

If the H_∞ mixed sensitivity control algorithm is the product of positive thinking, the loop-shaping algorithm can be said to be the product of divergent thinking, and the concise robust control algorithm based on closed-loop gain-shaping is the product of reverse thinking.

The typical S/T Singular Value (SV) curve is shown in Figure 2. To make the system robust and stable, the closed-loop spectrum of the system is required to be low-pass, and the maximum singular value is set to 1 to ensure the tracking of the reference signal without static error; the bandwidth of the system determines the control performance of the system, and the closing-door slope rate of the spectrum determines the sensitivity of the system to the interference outside the invalid frequency band. The larger the slope, the less sensitive the influence on the interference, and the stronger the robustness of the system. However, if the slope of the closing door is too large, the order of the controller is too high, which is not practicable for the realization of the controller. Generally speaking, the slope of door-closing can be set as -20 dB/dec, -40 dB/dec, and -60 dB/dec.

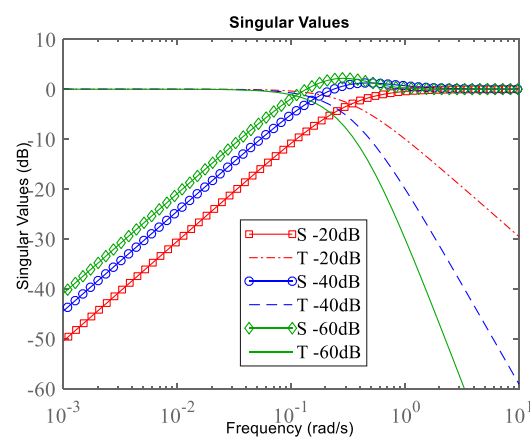


Figure 2. Typical singular value for S/T .

Assuming that the door-closing slope of the closed-loop system transfer function spectrum is -20 dB/DEC, the singular value curve of the complementary sensitivity function T is approximately expressed as the spectrum curve of the first-order inertial system with the maximum singular value of 1:

$$\frac{1}{Ts + 1} = \frac{GK}{1 + GK} \tag{7}$$

If the bandwidth of the closed-loop system is $1/T$, then the controller is

$$K = \frac{1}{GTs} \tag{8}$$

If the door-closing slope of the closed-loop system transfer function spectrum is -40 dB/DEC, the singular value curve of T is approximately expressed as the spectrum curve of the second-order inertial system with the maximum singular value of 1. Compared with the typical oscillation process, this is equivalent to the case where the damping coefficient is 1, thus ensuring that the spectrum of T has no peak for all door-closing slopes:

$$\frac{1}{(Ts + 1)^2} = \frac{GK}{1 + GK} \tag{9}$$

The controller is obtained as

$$K = \frac{1}{GTs(Ts + 2)} \tag{10}$$

For -60 dB/DEC, we have:

$$\frac{1}{(Ts + 1)^3} = \frac{GK}{1 + GK} \tag{11}$$

and the controller is:

$$K = \frac{1}{G[(Ts + 1)^3 - 1]} \tag{12}$$

4.2. Nominal Model for Control Law Design

At present, the nonlinear mathematical model of ship motion control is commonly used. The model has a simple form and few parameters, which can also basically reflect the nonlinear characteristics of the ship turning. However, it can only reveal the relationship between rudder angle and yawing, which cannot reflect the influence of the ship's velocity on yawing, hence limiting its application range.

In practical application, ship motion attitude is often considered in the design of ship motion controllers, so it is necessary to study the design of a ship controller with multiple degrees of freedom. In other words, the longitudinal and the lateral velocity of the ship should be considered at least.

The transformation of the terms f_3 in the Abkowitz model as mentioned in Equation (6) is carried out, and the terms include δ , and higher-order terms including $N_{\delta\delta\delta}\delta^3$, $N_{v\delta\delta}v\delta^2$, $N_{r\delta\delta}r\delta^2$ are ignored in the control law design, as they exert a minor influence on the final result, the parameter could be found in Table A1 in the Appendix A. Assume that:

$$f_3(u, v, r, \delta) = N_1 + N_2\delta \tag{13}$$

Among them:

$$\begin{cases} N_1 = N_0 + N_u\Delta u + N_{uu}\Delta u^2 + N_{uuu}\Delta u^3 + N_vv \\ \quad + N_r r + N_{vvv}\Delta v^3 + N_{rrr}\Delta r^3 + N_{vvr}v^2r \\ \quad + N_{vrr}vr^2 + N_{vu}v\Delta u + N_{ru}r\Delta u - mx_G r\Delta u \\ \quad + N_{vu}v\Delta u^2 + N_{ruu}r\Delta u^2 \\ N_2 = N_\delta + N_{v\delta}v\delta + N_{r\delta}r\delta + N_{v\delta}vr + N_{\delta u}\Delta u + N_{\delta uu}\Delta u^2 \end{cases} \tag{14}$$

N_1 and N_2 are nonlinear terms related to ship motion.

In 1965, Chislett carried out comprehensive research on "mariner" by Planar Motion Mechanism (PMM); the hydrodynamics of the vessel were obtained. The result had good conformity with the sea trial results in ship steady-turning and zigzag experiments. The parameters of the mariner are presented in Table 1.

Table 1. Parameters of the mariner.

Parameter	Value	Parameter	Value
Length of all L_{oa}	171.80	Volume of displacement ∇ (m ³)	18,541.00
Length between perpendiculars L_{pp} (m)	160.93	Rudder area A_R (m ²)	30.01
Breadth B (m)	23.17	Height of rudder H (m)	4.05
Designed draught d (m)	8.23	Diameter of propeller D_p (m)	6.706

With the purpose of verifying the influence on the simplification of δ and related terms, the steady-turning and the zigzag tests are conducted for the nominal model as described by Equation (13). Meanwhile, the simulation result is compared with the result from Chislett as well as the sea trial results.

As illustrated in Figure 3, the result of 2 the 0°/20° zigzag test is plotted. This refers to the results from Chislett, our simulation results, and sea trial results, respectively. It can be observed that the turning rate starts to increase under the rudder angle. The rudder starts to revert once the course reaches its target value. The course continues to increase due to the huge inertial of the ship even with the rudder reverted, but the course starts to revert until the turning rate decrease to zero. As indicated by the fact that our nominal model agrees with the result from Chislett and the sea trial results, the nominal model is close to the original Abkowitz model even if the δ -related higher-order terms are ignored, as shown in Equation (13).

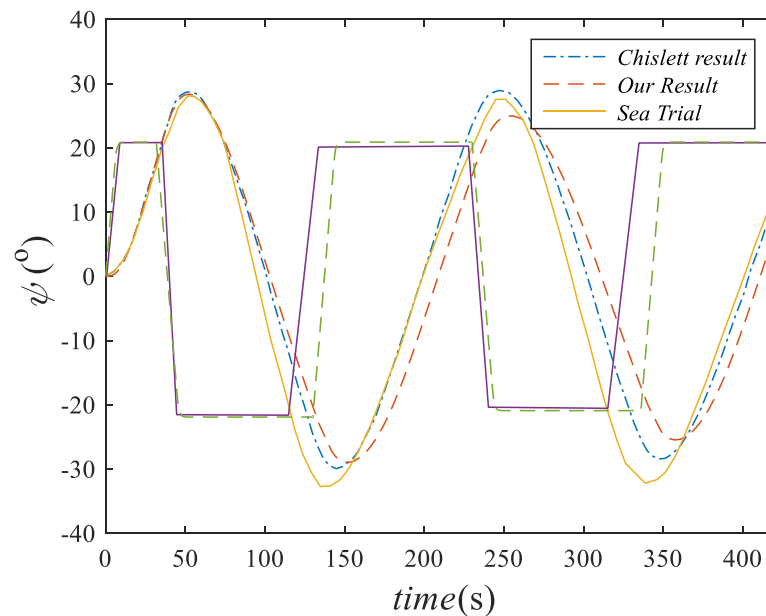


Figure 3. Comparison of zigzag test results (velocity of 15 kn).

The steady-state turning test is carried out at a rudder angle of 5°, 10°, 20° for both starboard and port side, and the results are shown in Figure 4. It is clear that the turning process includes the transition stage and steady-turning stage. In the transition stage, the ship starts yawing under the rudder angle applied; then, the turning rate reaches the maximum. After this, the turning rate begins to decrease slightly; shortly after, the turning rate becomes steady at around 200 s, and the ship begins a steady-state turning process.

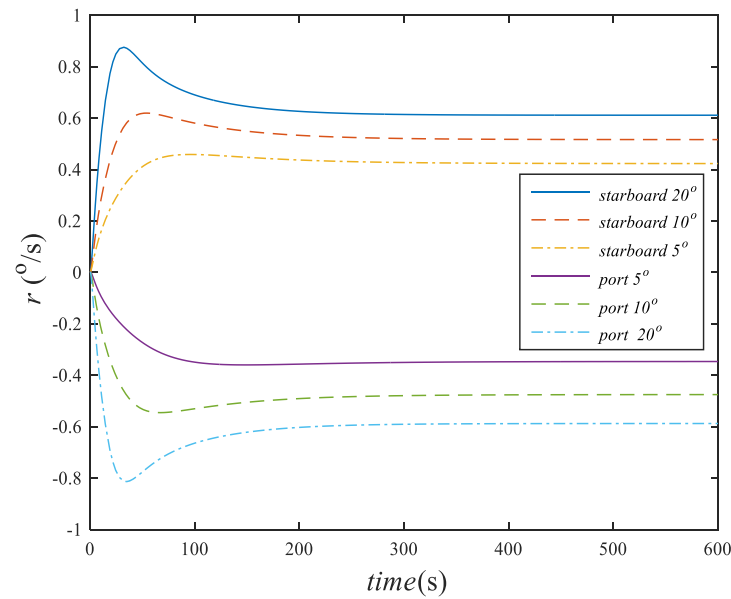


Figure 4. Steady-state turning test (velocity of 15 kn).

As shown in Figure 5, the mariner’s steady-state turning test is established in line with the Abkowitz model. The test has been carried out several times in the range of $[-20,20]$ degree rudder angle with 4° rudder angle interval. Among the above results, the simulation results of Chislett [27], the simulation results of our model in this paper, and the ship trial results are shown. It can be seen from the above results that the simulation results of our model are basically consistent with the simulation results of Chislett [27] and are close to the ship trial results of the real ship, which can reveal the basic characteristics of the actual ship. It should be noted that the simplified model is only used for the design of control law, also known as the nominal model, while the original Abkowitz ship motion model is called the perturbation model.

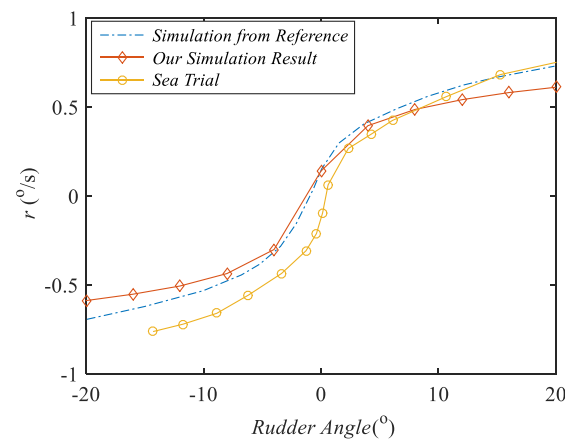


Figure 5. Steady-state turning of mariner (velocity of 15 kn).

4.3. Design of Nonlinear Ship Course Controller Based on Backstepping

The mathematical model of ship motion has a certain nonlinearity, and the backstepping method can deal with the nonlinear term effectively. The Lyapunov function of the whole system is constructed recursively through the structural characteristics of the system, which solves the problem that the Lyapunov method lacks the construction method. Moreover, it does not eliminate all the nonlinear terms of the system as other feedback methods do so that the designed controller is both flexible and robust. Moreover, it can reduce the control difficulty and energy consumption of the system.

The backstepping method and precise feedback linearization method are constructed by introducing nonlinear feedback or coordinate transformation, but the backstepping method constructs the Lyapunov function and stabilization controller simultaneously through the systematization method, so as to avoid eliminating the nonlinear term of the system. It can also overcome the shortcoming that the precise feedback linearization method needs an accurate system of the mathematical model.

Define:

$$\begin{cases} z_1 = \psi - \psi_d \\ z_2 = r \end{cases} \quad (15)$$

where

$$\dot{r} = f_3 = N_1 + N_2\delta \quad (16)$$

Define the Lyapunov function:

$$V = \frac{1}{2}k_1z_1^2 + \frac{1}{2}z_2^2 \quad (17)$$

Yield:

$$\begin{aligned} \dot{V} &= k_1z_1\dot{z}_1 + z_2\dot{z}_2 \\ &= k_1z_1(\dot{r} - \dot{\psi}_d) + z_2\dot{r} \\ &= k_1z_1(z_2 - r_d) + z_2\dot{r} \end{aligned} \quad (18)$$

where ψ_d and r_d are the setting course and its derivatives, respectively. In navigation practice, since the target course ψ_d to be tracked is usually a fixed value or its change is slow, it is assumed that $r_d = 0$ here. It should be noted that although this assumption is made here, it was found in the subsequent course tracking test that this method can also realize the course tracking control for the case $r_d \neq 0$. By substituting Equation (16) into Equation (18), we obtain the following results:

$$\begin{aligned} \dot{V} &= k_1z_1(z_2 - r_d) + z_2(\dot{r} + k_1z_1 - k_1z_1 + k_2z_2 - k_2z_2) \\ &= k_1z_1z_2 + z_2(N_1 + N_2\delta + k_1z_1 + k_2z_2 - k_1z_1 - k_2z_2) \end{aligned} \quad (19)$$

Assuming:

$$N_1 + N_2\delta + k_1z_1 + k_2z_2 = 0 \quad (20)$$

Then, the control law is obtained:

$$\delta = -\frac{1}{N_2}[N_1 + k_1z_1 + k_2z_2] \quad (21)$$

Yield:

$$\dot{V} = -k_2z_2^2 \quad (22)$$

where $k_1, k_2 > 0$ is the feedback coefficient. Thus, for $z_2 \neq 0$; hence:

$$\dot{V} < 0 \quad (23)$$

In this case, the system can be stabilized.

5. Simulation Experiments and Result Analysis

5.1. Nonlinear Ship Course-Keeping Experiment Results and Analysis

Without considering the disturbance of wind and waves, the results of ship course-keeping control by the different methods are shown in Figures 6 and 7. The target course is 30 degrees. The step curves of 0–2000 s are the results of a door-closing slope of -20 dB, -40 dB, -60 dB under PID control. From 400 s to 2000 s in Figure 7, the overlay results of the first 400 s of the corresponding rudder angle are plotted. It can be seen that the control performance of the CROB method with a -20 dB door-closing slope is close to that of PID control. However, the rudder angle is larger and the response is faster; the rudder angle

decreases gradually with the increase in the door-closing slope, and the system response also decreases. If the door-closing slope is -60 dB, the maximum rudder angle is less than 20° . As a result, under the same conditions, increasing the door-closing slope is beneficial to decrease the maximum rudder angle. Thus, it can improve navigation safety to a certain extent. In particular, when the vessel is at high-speed navigation, instantaneous application of a large rudder angle should be avoided. In this paper, all the simulation are carried out on Matlab 2015 with the Simulink toolbox, on a 64-bit Windows 10 operating system.

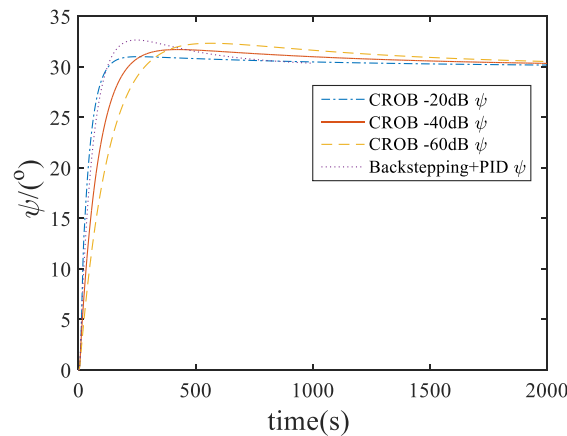


Figure 6. Comparison of CROB and PID based on backstepping.

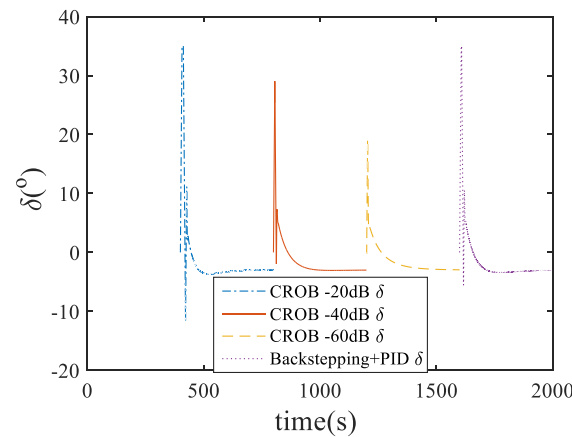


Figure 7. Rudder angle comparison of CROB and PID based on backstepping (the first 500 s).

5.2. Course-Tracking Experiment and Analysis

Figure 8 is the result of dynamically tracking course change with the target course defined by $10\sin(2\pi/100)$. It can be seen from the results that the PID control and CROB control based on backstepping can effectively track the target course.

At approximately 30 s, the course has been tracked after a short adjustment. Moreover, the rudder angle also shows a certain periodic law compared with the periodic course. However, due to the large inertia of the ship, there is a certain delay between the maximum rudder angle and the maximum course. Hence, the influence of the target course derivative is ignored in the course control law design, as described in Equation (21), but the effective tracking of the dynamic change course can still be achieved for a certain period (200 s).

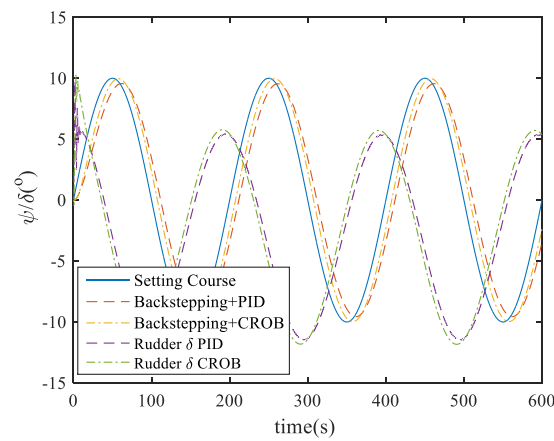


Figure 8. Comparison of dynamic course tracking.

5.3. Nonlinear Ship Robust Course-Keeping Control Experiment Results and Analysis in Case of Wind and Wave Disturbance

Under the wind interference with Beaufort scale 6, the control result of ship course-keeping is described in Figures 9 and 10, and the details of wind and wave are shown in reference [24,25]. The target course is set at 30°. The maximum rudder angles are 35°, 32.4°, 23.4°, and 35°, respectively. Compared with PID control, the maximum rudder angle is decreased by 7.4% and 33.2% when the CROB method with a door-closing slope of −40 dB and −60 dB, respectively, is used. Therefore, it can be observed that an increase in the door-closing slope can effectively reduce the maximum rudder angle.

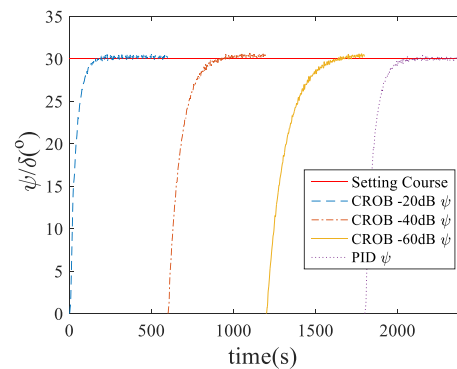


Figure 9. Concise robust control in case of wind-wave disturbance (scale 6).

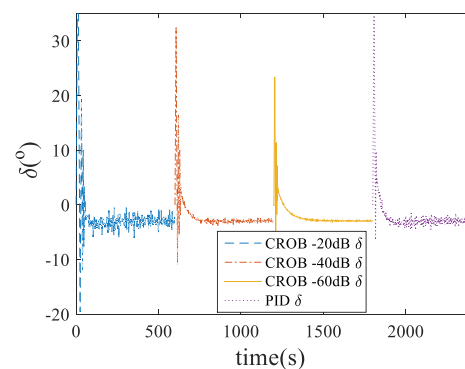


Figure 10. Rudder angle comparison under concise robust control and PID in case of wind and wave disturbance.

In the stable condition (500 s–1000 s), the maximum rudder angle, average rudder angle, rudder angle variance, and the time to the target heading of different control methods

are shown in Table 2, which shows that: ① the applied average rudder angle is 2.95° , which is consistent with the reference [24,25] with a 3° rudder angle; ② with the increase in the door-closing slope, the concise robust control algorithm can reduce the maximum rudder angle and rudder angle variance under wind–wave interference, achieving the goal of reducing the rudder wear and energy consumption.

Table 2. Concise robust control with wind–wave disturbance (500 s–1000 s).

Control Method	Max Rudder Angle ($^\circ$)	Avg Rudder Angle ($^\circ$)	Variance of Rudder Angle	Time to 95% Target Course (s)
CROB –20 dB	5.68	–2.94	5641.30	110.06
CROB –40 dB	3.61	–2.95	90.45	209.09
CROB –60 dB	3.20	–2.95	19.81	303.00
PID	4.56	–2.95	3189.80	154.90

However, in practice, a larger the door-closing slope does not yield better results. For example, the maximum rudder angle is 5.68° , 3.61° , and 3.20° in the concise robust control algorithm, while the relative maximum rudder angle decreased by 36% and 11% for –40 dB and –60 dB door-closing slopes, respectively, as shown in Table 2; the rudder angle variance is decreased by 61.4 times and 3.6 times, while the time to the target heading basically changes linearly (110 s, 209 s, 303 s). In other words, when the door-closing slope is increased from –20 dB to –40 dB, the maximum rudder angle is decreased by 36%, and the rudder angle variance is reduced by 61.4 times; correspondingly, the maximum rudder angle is decreased by 11% when the closing slope is increased from –40 dB to –60 dB, and the rudder angle variance is only decreased by 3.6 times. Therefore, the cost performance of the –40 dB door-closing slope is higher than –60 dB.

Compared with the PID method, the maximum rudder angle and rudder angle variance of –40 dB and –60 dB door-closing slopes are reduced by 20.9% and 34 times and by 29.8% and 160 times, respectively. It can be seen that although the PID method based on backstepping can realize the course control, the rudder angle variance and maximum rudder angle are too large to deal with the disturbance of wind and waves effectively. The concise robust control algorithm can select the appropriate frequency and door-closing slope according to the requirement in suppressing the wave interference, which can effectively reduce the maximum rudder angle and rudder angle variance, hence reducing the rudder wear and energy consumption.

6. Conclusions

In this paper, the 3DOF ship course control method based on concise robust control was proposed, and the concise robust control algorithm was constructed on the grounds of the closed-loop gain-shaping algorithm, and the stability should be a guarantee thanks to the Lyapunov function. The ship course controller designed here has the ability to deal with the model perturbation, implying that this method could suppress disturbances including wind and wave under environmental uncertainty. The limitations of the study and additional studies required in the future are to carry out a ship trial test on a real ship, in order to verify the robustness further.

(1) In this paper, the ability of concise robust control of model perturbation was verified. The control law designed according to the nominal model could effectively stabilize the perturbed model. The controller could not only realize the course keeping control but could also realize the tracking control of a continuously changing course periodically.

(2) In this paper, the ability for concise robust control in suppressing environmental disturbance such as wind and wave was validated. The disturbance of wind and wave with scale 6 interference on the ship’s course could be effectively suppressed by designing a door-closing slope for the closed-loop transfer function in the frequency domain. Compared

with the PID method based on backstepping, the rudder angle of steering gear could be significantly reduced and the wear of steering gear could be decreased significantly.

(3) Keeping other conditions the same, the larger the closing slope of the closed-loop transfer function spectrum is, the stronger its resistance to external interference, but its sensitivity will also decrease accordingly. Therefore, it is necessary to select the proper door-closing slope of the closed-loop transfer function spectrum according to the actual situation.

Author Contributions: Conceptualization, C.Z. and J.Y.; Methodology, C.Z. and J.Y.; Validation, C.Z. and Y.G.; formal analysis, C.Z. and Y.G.; visualization, Y.G.; Software, C.Z. and Y.G.; Investigation, C.Z. and Y.G.; writing—review and editing, C.Z., J.Y., and Y.G. All authors have read and agreed to the published version of the manuscript.

Funding: This research was funded by the National Natural Science Foundation of China (Nos. 61861017, 52062016, U2001213, 61971191, and 61661021), Key R & D Projects of Jiangxi Province (No. 20192ACB50027), Jiangxi Science and Technology Transportation Department Project (No. HX2019-332), Key Projects of Jiangxi Provincial Department of Education(No. GJJ190296), Key R & D Projects of Jiujiang City (No. 20200069), Beijing Natural Science Foundation under Grant L182018 and L201011, National Key Research and Development Project (No. 2020YFB1807204), open project of Shanghai Institute of Microsystem and Information Technology (No. 20190910), the Key project of Natural Science Foundation of Jiangxi Province (No. 20202ACBL202006), Provincial Teaching Reform Research Key Project of Jiangxi Province (No. JXJG-20-5-3), Teaching Reform Project of Electronic Information Specialty Teaching Steering Committee (No. 2020-YB-55), Teaching Reform Research Project of Degree and Postgraduate Education in Jiangxi Province (No. JXYJG-2020-107).

Institutional Review Board Statement: Not applicable.

Informed Consent Statement: Not applicable.

Data Availability Statement: The data presented in this study are available on request from the corresponding authors.

Conflicts of Interest: The authors declare no conflict of interest.

Appendix A

Table A1. Hydraulic coefficients for mariner.

$X_{\dot{u}} = -42 \times 10^{-5};$	$Y_{\dot{v}} = -748 \times 10^{-5};$	$N_{\dot{v}} = 4.646 \times 10^{-5};$
$X_u = -184 \times 10^{-5};$	$Y_{\dot{r}} = -9.354 \times 10^{-5};$	$N_{\dot{r}} = -43.8 \times 10^{-5};$
$X_{uu} = -110 \times 10^{-5};$	$Y_v = -1160 \times 10^{-5};$	$N_v = -264 \times 10^{-5};$
$X_{uuu} = -215 \times 10^{-5};$	$Y_r = -499 \times 10^{-5};$	$N_r = -166 \times 10^{-5};$
$X_{vv} = -899 \times 10^{-5};$	$Y_{vv} = -8078 \times 10^{-5};$	$N_{vv} = 1636 \times 10^{-5};$
$X_{rr} = 18 \times 10^{-5};$	$Y_{vr} = 15356 \times 10^{-5};$	$N_{vr} = -5483 \times 10^{-5};$
$X_{dd} = -95 \times 10^{-5};$	$Y_{vu} = -1160 \times 10^{-5};$	$N_{vu} = -264 \times 10^{-5};$
$X_{udd} = -190 \times 10^{-5};$	$Y_{ru} = -499 \times 10^{-5};$	$N_{ru} = -166 \times 10^{-5};$
$X_{rv} = 798 \times 10^{-5};$	$Y_d = 278 \times 10^{-5};$	$N_d = -139 \times 10^{-5};$
$X_{vd} = 93 \times 10^{-5};$	$Y_{ddd} = -90 \times 10^{-5};$	$N_{ddd} = 45 \times 10^{-5};$
$X_{uvd} = 93 \times 10^{-5};$	$Y_{ud} = 556 \times 10^{-5};$	$N_{ud} = -278 \times 10^{-5};$
	$Y_{uud} = 278 \times 10^{-5};$	$N_{uud} = -139 \times 10^{-5};$
	$Y_{vdd} = -4 \times 10^{-5};$	$N_{vdd} = 13 \times 10^{-5};$
	$Y_{vvd} = 1190 \times 10^{-5};$	$N_{vvd} = -489 \times 10^{-5}$
	$Y_0 = -4 \times 10^{-5};$	$N_0 = 3 \times 10^{-5};$
	$Y_{0u} = -8 \times 10^{-5};$	$N_{0u} = 6 \times 10^{-5};$
	$Y_{0uu} = -4 \times 10^{-5};$	$N_{0uu} = 3 \times 10^{-5};$

References

1. Zhang, X.K.; Jai, X.L. *Ship Motion Control*; National Defense Industry Press: Beijing, China, 2006.
2. Amerongen, J.V.; Udink Cate, A.L. Model reference adaptive autopilots for ships. *Automatica* **1975**, *11*, 441–450. [[CrossRef](#)]
3. Amerongen, J.V. Adaptive Steering of Ship—a Model Reference Approach to Improved Maneuvering and Economical Course-Keeping. Ph.D. Thesis, Delft University of Technology, Delft, The Netherlands, April 1982.
4. Chen, X.; Zhao, H.; Zhen, S.; Sun, H. Adaptive Robust Control for a Lower Limbs Rehabilitation Robot Running Under Passive Training Mode. *IEEE/CAA J. Autom. Sin.* **2019**, *6*, 160–169. [[CrossRef](#)]
5. Ozbek, C.; Ozguney, O.C.; Burkan, R.; Yagiz, N. Design of a fuzzy robust-adaptive control law for active suspension systems. *Sādhanā* **2020**, *45*, 1–16. [[CrossRef](#)]
6. Ohtsu, K.M. A new ship's autopilots design through a stochastic model. *Automatica* **1979**, *115*, 255–268. [[CrossRef](#)]
7. Kallstrom, C.G.; Astrom, K.J. Adaptive autopilots for tanker. *Automatica* **1979**, *15*, 241–254. [[CrossRef](#)]
8. Kallstrom, C.G.; Norrbin, N.H. Performance criteria for optimum steering of ships. In Proceedings of the Symposium on Ship Automatic Control, Genova, Italy, 25–27 June 1980.
9. Tzeng, C.Y.; Goodwub, G.C.; Criafulli, S. Feedback linearization of a ship steering autopilot with saturating and slew rate limiting actuator. *Int. J. Adapt. Control Signals Process.* **1999**, *13*, 23–30. [[CrossRef](#)]
10. Hu, Y.H.; Jia, X.L. Application of generalized predictive control to ship course and track keeping. *Ship Build. China* **1998**, *1*, 36–41.
11. Hu, Y.H.; Jia, X.L. Predictive control of ship motion. *J. Dalian Marit. Univ.* **1998**, *24*, 5–9.
12. Katebi, M.R. LQR adaptive ship autopilot. *Trans. Inst. MC* **1988**, *10*, 187–197. [[CrossRef](#)]
13. Peng, X.Y.; Zhao, X.R.; Yin, Z.F. Statistical analysis of robustness of LQG control for ship lateral motion. *J. Syst. Simul.* **2007**, *19*, 250–254.
14. Fossen, T.I.; Strand, J.P. Nonlinear Ship Control (Tutorial Paper). In Proceedings of the IFAC Conference on Control Application in Marine Systems CAMS', Fukuoka, Japan, 27–30 October 1998; pp. 1–75.
15. Fossen, T.I. *Marine Control Systems: Guidance, Navigation and Control of Ships, Rigs and Underwater Vehicles*; Marine Cybernetics: Trondheim, Norway, 2002.
16. Fossen, T.I. *Handbook of Marine Craft Hydrodynamics and Motion Control*; Wiley: New York, NY, USA, 2011.
17. Wu, J.C.; Agraval, A.K.; Yang, J.N. Application of sliding model control to benchmark problem. In Proceedings of the ASCE Structures Congress, Portland, OR, USA, 13–16 April 1997.
18. Healey, A.J.; Lineard, D. Multivariable sliding model control for autonomous diving and steering of unmanned underwater vehicles. *IEEE J. Ocean. Eng.* **1993**, *18*, 327–339. [[CrossRef](#)]
19. Liu, W.J. *Nonlinear Control of Ship Course and Track*; China Water and Power Press: Beijing, China, 2019.
20. Lin, Y.Y. Study of Ship Course Nonlinear Control Based on Backstepping. Master's Thesis, Dalian Maritime University, Dalian, China, 2007.
21. Witkowska, A.; Śmierczalski, R. A New Approach of Genetic Algorithms to Tuning Parameters of Backstepping Ship Course Controller. *Pr. Nauk. Politech. Warsz. Elektron.* **2007**, *160*, 301–307.
22. Yan, Z.K.; Zhang, X.K.; Zhu, H.Y. Course-keeping control for ships with nonlinear feedback and zero-order holder component. *Ocean Eng.* **2020**, *209*, 1–14. [[CrossRef](#)]
23. Hu, S.S.; Yang, P.H.; Juang, J.Y.; Chang, B.C. Robust nonlinear ship course-keeping control by H_∞ I/O linearization and μ -synthesis. *Int. J. Robust Nonlinear Control* **2003**, *13*, 55–70. [[CrossRef](#)]
24. Zhang, X.K.; Yang, G.; Zhang, Q.; Zhang, G.; Zhang, Y. Improved concise backstepping control of course keeping for ships using nonlinear feedback technique. *J. Navig.* **2017**, *70*, 1401. [[CrossRef](#)]
25. Zhang, Q.; Zhang, X.K. Nonlinear improved concise backstepping control of course keeping for ships. *IEEE Access* **2019**, *7*, 19258–19625. [[CrossRef](#)]
26. Do, K.D. Global robust adaptive path-tracking control of underactuated ships under stochastic disturbances. *Ocean Eng.* **2016**, *111*, 267–278. [[CrossRef](#)]
27. Chislett, M.S.; Strom-Tejsen, J. Planar motion mechanism tests and full-scale steering and manoeuvring predictions for a Mariner class vessel. *Int. Shipbuild. Prog.* **1965**, *12*, 201–224. [[CrossRef](#)]